

Analysis And Selection Of Airfoil For A Fixed-Wing Unmanned Aerial Vehicle

Olukunle K. Soyinka¹, Ahmad K. Hussain², Luka L. Joshua²

¹*Department Of Aerospace Engineering, Institute Of Space Science And Engineering, Affiliate Of African University Of Science And Technology, Abuja, Nigeria.)*

²*Aeronautics Division, Department Of Engineering And Space Systems, National Space Research And Development Agency, Abuja, Nigeria.)*

Abstract

Four Eppler series airfoils were studied in a design project for a wing airfoil of a 7.5kg fixed-wing Unmanned Aerial Vehicle with an estimated maximum coefficient of lift of 1.66. Two high-lift airfoils and two general aviation airfoils were analyzed based on the conceptual design requirements and the aerodynamic characteristics of the airfoils were estimated. XFLR5 software was used for the airfoil analysis. The performance coefficients of lift, drag, pitching moment and lift-to-drag ratio coefficients were estimated for the angle of attack ranging from -20° to $+20^\circ$. The most suitable airfoil for a better lifting capacity, reduced drag and good stalling properties was selected for the wing development. ANSYS Fluent was used to analyze the suitable airfoil and the velocity and pressure distribution over the airfoil shows a smooth generation along the chord at both zero angle of attack and the wing incidence angle (4.05°). The simulation results were used to verify the results of the XFLR5 analysis.

Key Words: Airfoils, Fixed-Wing, Aerodynamic Characteristics, Unmanned Aerial Vehicles

Date of Submission: 15-02-2025

Date of Acceptance: 25-02-2025

I. Introduction

In recent years, Unmanned Aerial Vehicles (UAVs) have attracted the attention of researchers working on their development to improve their performance in various applications such as Agriculture, Military Operations, Surveillance, Atmospheric Research, Search and Rescue Operations, etc. Fixed-wing and rotary-wing systems are the two categories of UAVs that can be seen depending on the mission requirements [5].

Fixed-wing UAVs are advanced systems that are exclusively significant in terms of aerodynamics performance, maneuvering, load-carrying capabilities and performing stealth, military and commercial operations [8]. The wings are the main lifting components of the fixed-wing UAVs that provide the lift force. An effective wing design in line with the design and mission requirements of any UAV is critical to achieving the targeted flight performance. The cross-sectional shape of a wing (Two-dimensional), also termed an airfoil, is a key parameter that needs to be determined after estimating the characteristics of the UAV [9].

Several applications of airfoils are suitable for producing high lift at low Reynolds numbers. Such applications include wind turbine blades, airfoil selection of cross-flow fans, airfoils of sailplanes, and UAVs designed for fun flights and competitions [3]. Eppler series airfoils are suitable for velocity distributions in a subsonic local flow. They are coded based on a combined conformal mapping method with prescribed velocity distribution characteristics, a panel method for analysis of the potential flow about given airfoils, and an integral boundary layer method [4]. They are very efficient and have been successfully applied at Reynolds numbers ranging from 3×10^4 to 5×10^7 .

This study presents different criteria, conditions, and procedures for selecting a wing airfoil. The design brief and initial assumptions for the UAV design were defined for a maximum take-off weight of 7.5kg, cruise velocity of 15ms^{-1} , stall velocity of 9.6ms^{-1} , cruise altitude of 100m, service ceiling of 1000m and a target endurance of 2 hours.

II. Methodology

The aim of this research paper is to analyze and select a suitable airfoil for developing a mini fixed-wing UAV. The Reynold's number was estimated at the flight take-off, cruise, stalling and service ceiling conditions. Airfoil data are obtained from the airfoil database site for the analysis modeling in XFLR5 software. The analysis results were reviewed to select the most suitable wing airfoil for the design project. ANSYS Fluent

was used to simulate the performance of the selected airfoil. The results from Fluent simulation were used to verify the results from the XFLR5 analysis. The airfoil selection process is shown in Figure 1 below:

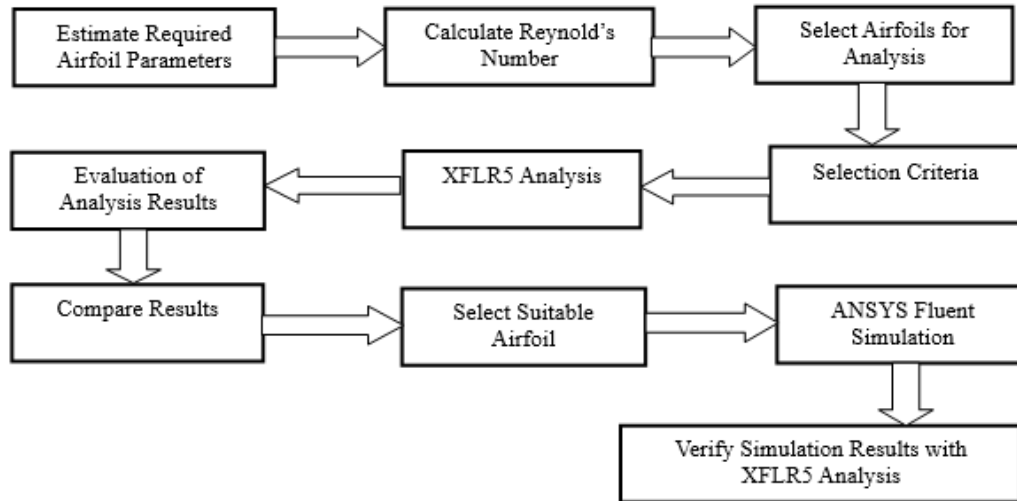


Figure 1: Airfoil analysis and selection process

Study Brief

Four Eppler airfoils were considered for analysis and selection of a suitable airfoil for wing development of a mini fixed-wing UAV. This study considered two Eppler general aviation application airfoils (E1210 and E1211) and two Eppler high-lift airfoils (E421 and E423). The conceptual UAV design data are a take-off weight (W_{TO}) of 7.5kg, cruise altitude of 100m, service ceiling of 1000m, cruise velocity (V_c) of 15ms^{-1} , take-off velocity (V_{TO}) of 12ms^{-1} and a stalling velocity (V_s) of 9.6ms^{-1} .

Aerodynamic characteristics parameters of the airfoils were estimated and compared using the XFOil analysis in XFLR5 software. The best-performing airfoil for the given inputs and with the highest rating was selected and analyzed using ANSYS Fluent for wing development. The lift coefficient (C_l), drag coefficient (C_d) and pitching moment coefficient (C_m) from the simulation result are used to verify the XFLR5 analysis.

Reynold's Number

The Reynold's number needs to be estimated before selecting an airfoil for analysis. Reynold's number helps to predict whether the fluid flow over an object is laminar or turbulent. A higher number means predominant turbulence because the fluid flow or object scale is large relative to the flow viscosity which can be estimated using the expression [1]:

$$Re = \frac{\rho * V * x}{\mu} \tag{1}$$

It also depends on flight altitude, temperature, viscosity, velocity, density and airfoil mean aerodynamic chord (MAC). The kinematic viscosity (ν) can also be calculated using [1]:

$$\nu = \frac{\mu}{\rho} \tag{2}$$

Where x is the characteristic length of the solid in which fluid flows, ρ is the density of the medium, V is the velocity of flow and μ is the dynamic viscosity of the medium.

Lift and drag are functions of flow Reynold's number (Re). A higher Re postpones the onset of stall (higher stall angle of attack) and implies a higher maximum lift coefficient ($C_{l_{max}}$) while a lower Re means early stall, lower $C_{l_{max}}$ and stall angle of attack (α_s) [6]. The Re and ν values from International Standards of Atmosphere (ISA) were calculated for take-off, cruise altitude, service ceiling and stalling conditions.

Table 1: Reynold's number and kinematic viscosity

Condition	V (m/s)	Altitude (m)	Re	ν (m ² /s)
Take-off	12	0	207158.02	1.796153E-05
Cruise	15	100	319261.98	1.796136E-05
Stalling	9.6	100	204327.67	1.796136E-05
Ceiling	15	1000	421406.45	1.795990E-05

The flow is turbulent at take-off, cruise, stalling and ceiling conditions due to higher Re as shown in Table 1 above.

Required Aerodynamic Characteristics of the Airfoil

The required aerodynamic properties of the airfoil were calculated based on the wing design data. An estimated wing area (S) = 0.778 m², W_{TO} = 7.5Kg, Span (b) = 2.495m, MAC = 0.32m, aspect ratio (AR) = 8, V_{TO} = 12ms⁻¹, V_c = 15ms⁻¹ and V_s = 9.6ms⁻¹ were used for the aerodynamic estimations.

Required cruise lift coefficient (C_{L_c}) [6]:

$$C_{L_c} = \frac{2 * W_{TO} * g}{\rho_c * V_c^2 * S} = 0.63 \tag{3}$$

Where ρ_c is the density at cruise altitude.

Required take-off lift coefficient ($C_{L_{TO}}$) [6]:

$$C_{L_{TO}} = 0.85 * \frac{2 * W_{TO} * g}{\rho * V_{TO} * S} = 0.911 \tag{4}$$

Here, ρ is the density at sea level.

Wing cruise lift coefficient ($C_{L_{c_w}}$) [6]:

$$C_{L_{c_w}} = \frac{C_{L_c}}{0.95} = 0.73 \tag{5}$$

Wing airfoil ideal lift coefficient (C_{l_i}) [6]:

The wing setting angle corresponds to this value when read from the C_l vs α plot.

$$C_{l_i} = \frac{C_{L_{c_w}}}{0.9} = 0.81 \tag{6}$$

UAV maximum lift coefficient ($C_{L_{max}}$) [6]:

$$C_{L_{max}} = \frac{2 * W_{TO} * g}{\rho * V_s^2 * S} = 1.66 \tag{7}$$

Wing maximum lift coefficient ($C_{L_{max_{w}}}$) [6]:

$$C_{L_{max_{w}}} = \frac{C_{L_{max}}}{0.95} = 1.75 \tag{8}$$

Wing airfoil gross maximum lift coefficient ($C_{l_{max_{gross}}}$) [6]:

$$C_{l_{max_{gross}}} = \frac{C_{L_{max_{w}}}}{0.9} = 1.94 \tag{9}$$

The gross maximum lift coefficient calculated above is with flaps. It is important to note a high lift device lift coefficient increment ($\Delta C_{L_{HLD}}$), which is the required lift coefficient increment during take-off and landing configurations. The lift coefficients range from 0.7 to 0.9 for plain flaps [6].

Assuming: $\Delta C_{L_{HLD}} = 0.7$

Calculate maximum wing airfoil lift coefficient ($C_{l_{max}}$) [6]:

$$C_{l_{max}} = C_{l_{max_{gross}}} - \Delta C_{L_{HLD}} = 1.24 \tag{10}$$

Airfoil Selection Criteria

Several airfoils are available on the airfoil Database site and following suitable criteria to select the best airfoil for a UAV wing; for better lift capacity of the airfoil, a safety factor needs to be inserted (say of 0.5) to keep the $C_{l_{max}}$ value above the theoretical $C_{l_{max}}$ during the airfoil selection for better lifting capacity [6]. That is:

$$C_{l_{max}} = 1.24 + 0.5 = 1.74$$

Hence, the airfoil $C_{l_{max}}$ should be greater than 1.74. The airfoil needs to be selected based on some parameters ranking as shown in table 2 below [6].

Table 2: Selection criteria for airfoil aerodynamic parameters

S/N	Parameter	Requirement
1	Cl	Maximum
2	Cd	Minimum
3	Cl/Cd	Maximum
4	Stall	Smooth nature
5	Cm	Close to zero

The Eppler airfoils have moderate camber and thickness; the camber should be greater than 5% of the chord, the thickness should be greater than 10% and a high $(C_l/C_d)_{max}$ value for a high take-off efficiency [2]. The airfoils selected for this study can be structurally reinforced and developed. The wing incidence angle ($\alpha_{incidence}$) is 4.05° for fixing on the fuselage and this provides safety due to stalling and a better lift distribution [6].

Airfoil Characteristics Graph Analysis

The airfoil characteristics parameters were estimated with XFOIL analysis using XFLR5 software version 6.59 for E1210, E1211, E421 and E423 airfoils. Analysis type-1 was used at Re 500000 while NCrit was set at 9.00. The angle of attack (α) range starts at -20° and finishes at 20° with an increment of 1° . 500 iterations were defined to perform the analysis.

C_l vs α

The highest value from the curves in Figure 2 is the $C_{l_{max}}$ which corresponds to α_s and where the lift efficiency will no longer increase with α [6]. The ideal coefficient of lift (C_{l_i}) is the C_l where C_d does not vary significantly with minor changes in α and where a low flight cost can be optimized. The slope of the curves in the linear region (C_{l_α}) indicates the capacity of the airfoil to produce lift, the higher the C_{l_α} , the better the airfoil [6].

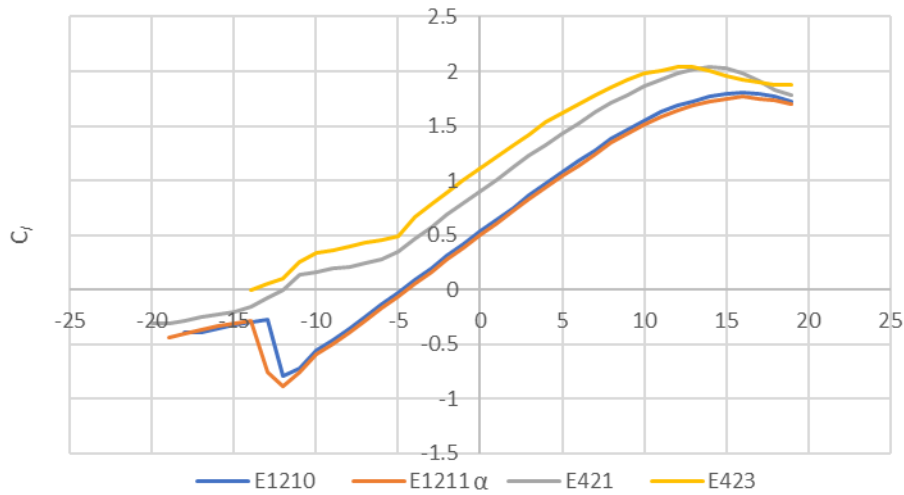


Figure 2: C_l vs α graph

C_m vs α

Figure 3 below shows the airfoils produce a negative C_m , a nose-down effect from the airfoil analysis. The C_m value strongly contributes to the aerodynamic longitudinal stability. A C_m value at zero α (C_{m_0}) of the airfoil closest to the origin signifies the more stable the airfoil for cruise flight [7]. The tail component nullifies the effect of the pitching moment and should be close to zero as far as possible to have equilibrium in flight[6].

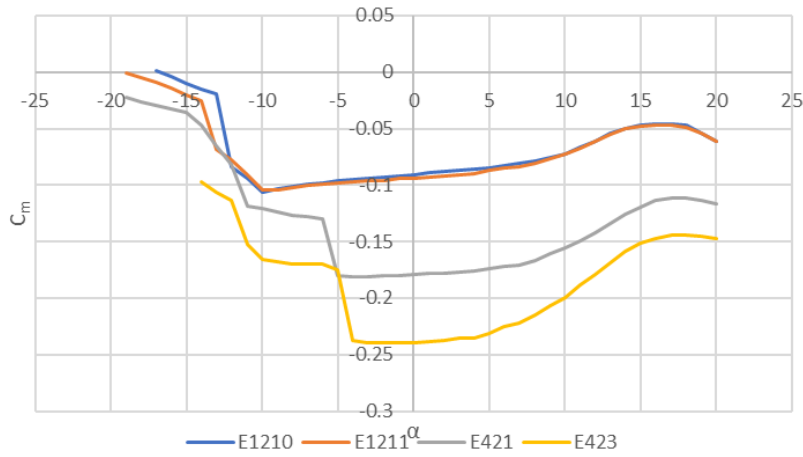


Figure 3: C_m vs α graph

C_l/C_d vs α

The extreme point of the curves in Figure 4 below indicates the maximum lift-to-drag ratio $(C_l/C_d)_{max}$. The value corresponds to the optimum design value of α [6].

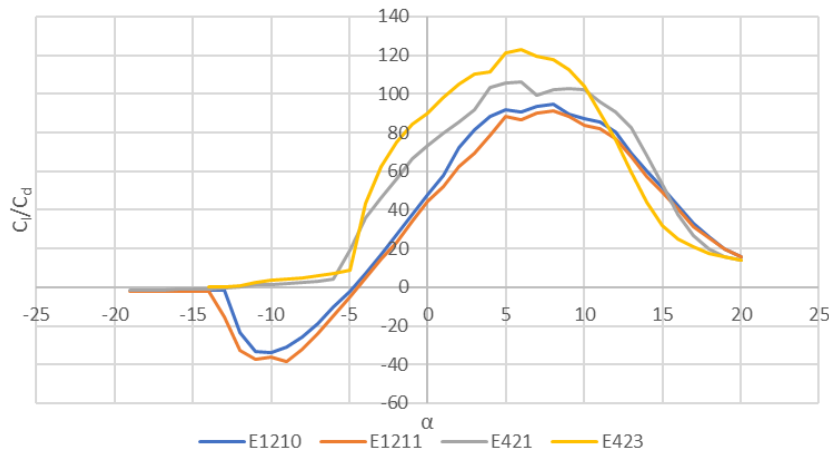


Figure 4: C_l/C_d vs α graph

C_d vs C_l

The minimum drag coefficient ($C_{d_{min}}$) is the lowest point in Figure 5 which corresponds to the minimum value of C_l ($C_{l_{min}}$) and the bucket shape of the lower region of the graph indicates that $C_{d_{min}}$ will not vary for a limited range of C_l [6]. This is the ideal design region where α can be varied without increasing drag.

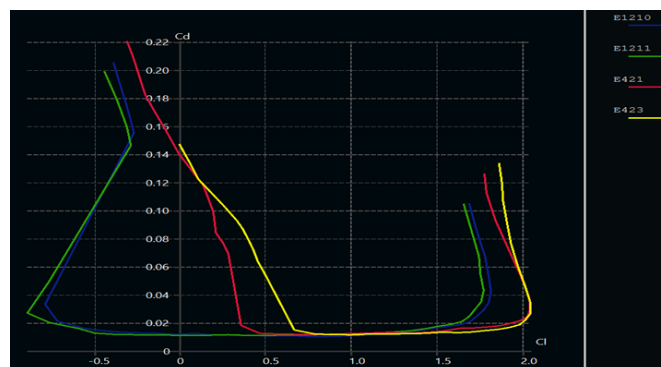


Figure 5: C_d vs C_l graph

III. Results And Analysis

The results from the airfoils performance curves and graphical analysis were obtained and the following observations were recorded as seen in Table 3 below:

Table 3: Airfoil analysis results (at $Re\ 500000$)

Parameter	Airfoils			
	E421	E423	E1211	E1210
$C_{d\ min}$	0.0121	0.0119	0.0120	0.0100
$C_{d\ 0}$	0.1445	0.1492	0.012	0.0124
$C_{l\ min}$	0.680	0.950	0.400	0.8580
$C_{l\ max}$	2.03	2.04	1.77	1.81
α_s (deg)	15	13	16	16
$(C_l/C_d)_{max}$	113	121	90	95
α_i at $C_{l_i} = 0.81$	-0.83	-2.70	2.83	2.575
α_0 (at $C_l = 0$)	-16	-13.83	-4.46	-4.788
$C_{l\ \alpha}$	0.1040	0.1004	0.1090	0.1071
$C_{m\ 0}$	-0.181	-0.240	-0.089	-0.086

Further study of the results and ranking of the performance of the airfoil based on some weighted design objectives yields the following results.

Table 4: Airfoils based on weighted design objectives

Design Objectives	Weight	E421	E423	E1211	E1210
$C_{d\ min}$	25%	22	22	22	23
$C_{m\ 0}$	20%	11	9	14	16
α_s	15%	13	12	15	15
α_0	5%	3	3	5	5
$(C_l/C_d)_{max}$	15%	14	15	9	10
Stall Quality	20%	10	10	20	19
Summation	100%	73	71	85	88
Stall (comment)		Sharp	Sharp	Docile	Moderate

The following observations are drawn from the results in Table 3 and 4 above:

- i. E1210 yields the highest maximum speed since it has the lowest $C_{d\ min}$ and less energy consumption in flight operations.
- ii. E1210 and E1211 yield the lowest stall speed since they have the highest α_s . This is an indication of a safer flight.
- iii. E423 yields the highest endurance since it has the highest $(C_l/C_d)_{max}$. It is also an indication of a better take-off performance.
- iv. E1211 yields the safest flight, due to their docile stall quality.
- v. E1210 delivers the lowest $C_{m\ 0}$ (closest to zero) which is an indication of equilibrium in cruise flight.

Due to the above reasons and the results in Table 4 above of weighted design objectives, E1210 was selected as the most suitable airfoil for the wing development.

ANSYS Fluent was used to simulate the performance characteristics of the airfoil. Analysis results at $\alpha=0^\circ$ and $\alpha=4.05^\circ$ are shown in Fig. 6, 7 and 8 for the convergence of C_d , C_l and C_m respectively.

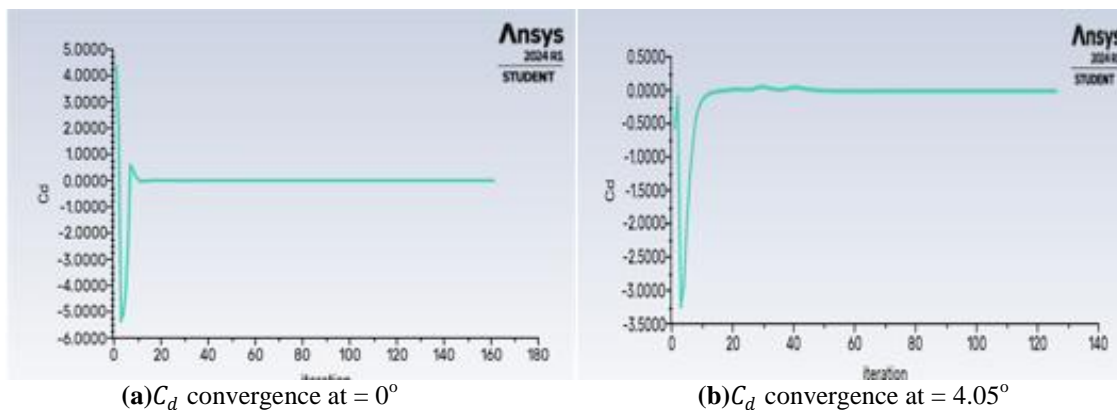


Figure 6: C_d convergence curve

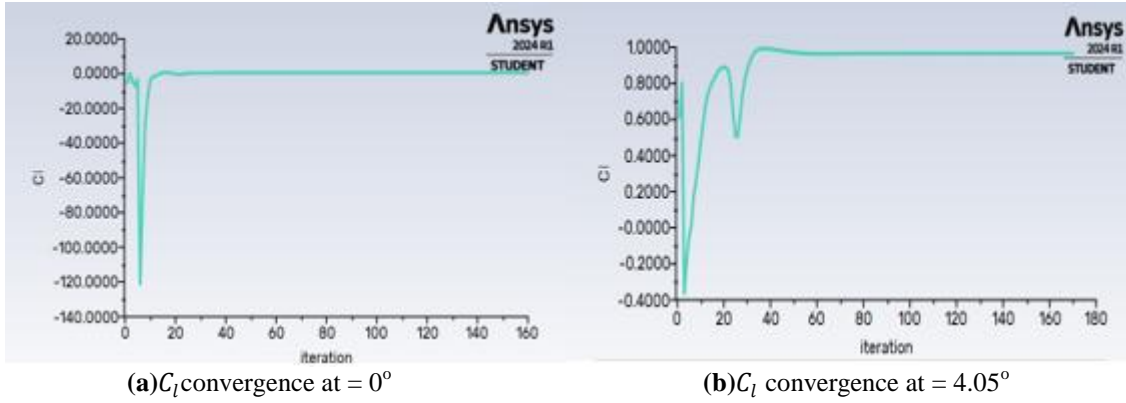


Figure 7: C_l convergence curve

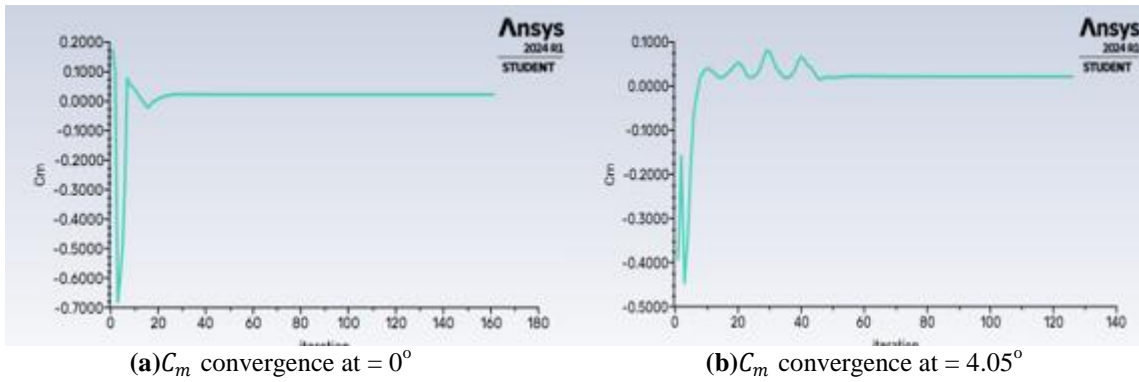


Figure 8: C_m convergence curve

The pressure distribution contours simulated over the airfoil are shown in Fig. 9 below at both the zero angle of attack and the wing airfoil incidence setting angle ($\alpha = 4.05^\circ$) respectively.

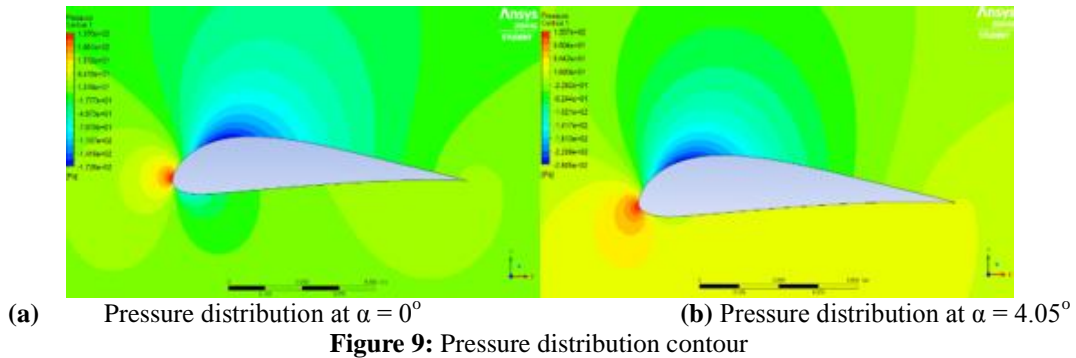


Figure 9: Pressure distribution contour

The velocity distribution contours simulated over the airfoil are also shown in Fig.10 below at both the zero angle of attack and the wing airfoil incidence setting angle respectively.

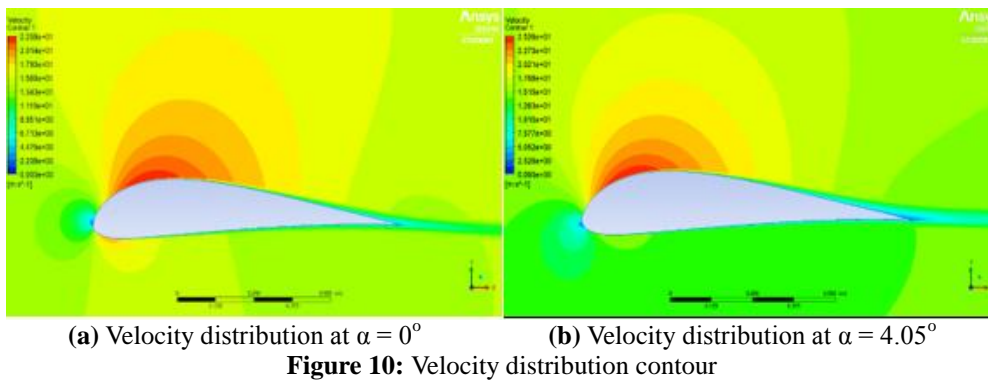


Figure 10: Velocity distribution contour

The velocity streamline flow simulated over the airfoil are also shown in Fig.11 below at both the zero angle of attack and the wing airfoil incidence setting angle respectively.

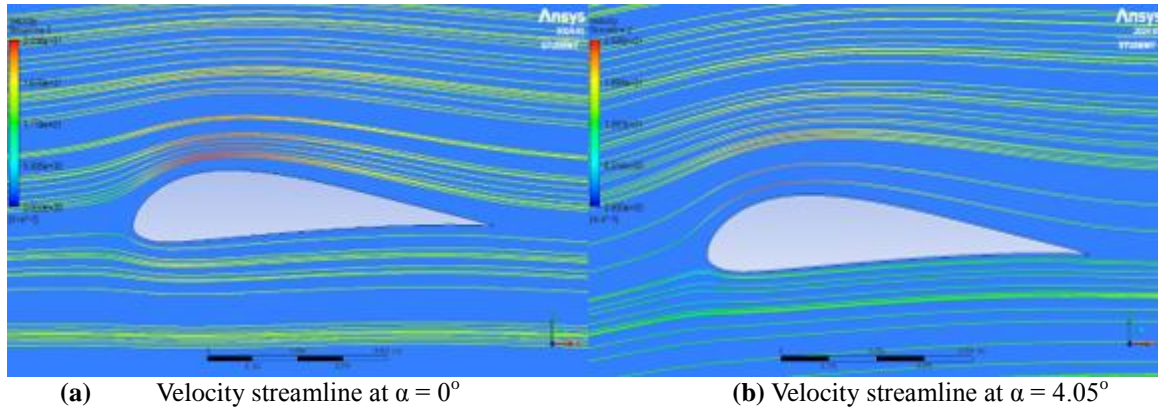


Figure 11: Velocity streamline over the airfoil

The simulations results for the E1210 airfoil were compared at both the zero and the wing incidence angle of attack and the parameters are as seen in the Fig. 12 below:

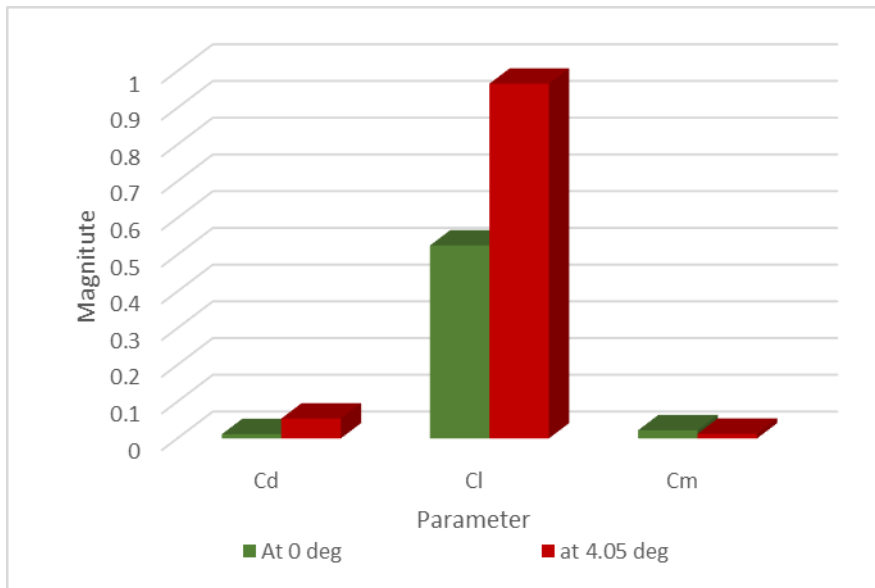
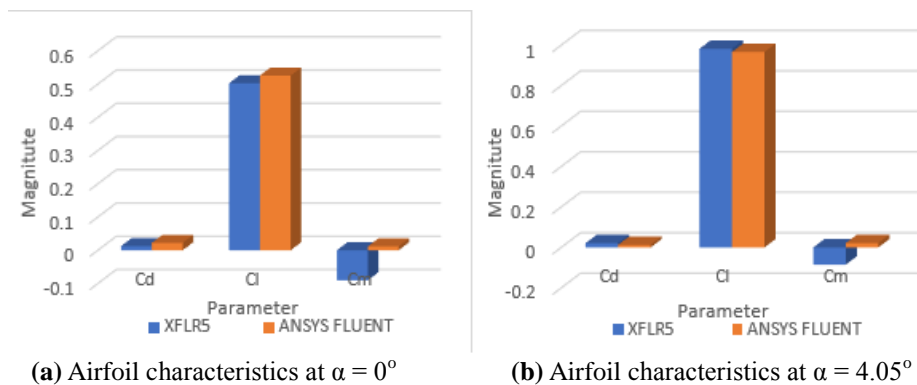


Figure 12: Airfoil simulation results

The convergence results for C_d , C_l and C_m from the ANSYS Fluent simulation are used to verify the XFLR5 airfoil model analysis at both the zero and the wing incidence angle of attack as shown in Fig. 13 below:



(a) Airfoil characteristics at $\alpha = 0^\circ$

(b) Airfoil characteristics at $\alpha = 4.05^\circ$

Figure 13: Airfoil characteristics validation

The four Eppler airfoils were analyzed and E1210 was selected as the most suitable for the required UAV wing design. The velocity and pressure distribution over airfoil profile generated from the ANSYS simulation shows that the upper surface and along the airfoil chord are smooth and change with a change in the angle of attack. The contours also show the airfoil has a good lift as predicted from the graph of the XFLR5 analysis. The C_d , C_l and C_m values at the wing incidence angle from the analysis were compared and both results indicate good lift characteristics of the airfoil. The selection process is part of a mini UAV design project. The selected airfoil and wing model using CATIA V5 can be seen in Figure 14 below.

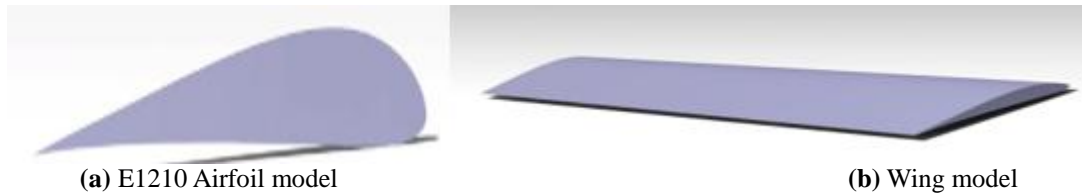


Figure 14: E1210 wing airfoil model

IV. Conclusion

The lifting force of a fixed-wing UAV is generated mainly by the wing component. Proper methodology for airfoil analysis and selection gives a better idea of the choice of the appropriate airfoil for wing development. The airfoil selection process was based on design requirements for the given UAV application. The present work elaborates on the various steps for effective airfoil selection and analysis. XFOIL analysis in XFLR5 and ANSYS Fluent were mainly used for this study. The aerodynamic performance characteristics generated from the analysis were majorly accepted with a good lift performance and limited drag.

References

- [1] Anderson J.D (2010) Aircraft Performance And Design. Tata Mcgraw Hill Education Private Limited, New Delhi, India.
- [2] Ashutosh R.K, Mohit S.D, Parikshit S.D, Babasaheb K.V (2022) Selection And Analysis Of An Airfoil For Fixed Wing Micro Unmanned Aerial Vehicle. International Research Journal Of Engineering And Technology. Vol 9, Iss 01.
- [3] Durmus S, Ulutas A (2021) Numerical Analysis Of NACA 6409 And Eppler 423 Airfoils. Journal Of Polytechnic, Turkey. ISSN: 2147-9429
- [4] Eppler R (1990) Airfoil Design And Data. Springer-Verlag Berlin Heidelberg GmbH. Doi:10.1007/978-3-662-02646-5.
- [5] Newcome L.R (2004) Unmanned Aviation: A Brief History Of Unmanned Aerial Vehicles. AIAA, Reston, Virginia.
- [6] Sadraey M.H (2013) Aircraft Design: A System Engineering Approach. WILEY & Sons Ltd, USA.
- [7] Sandapeta S.V, Parre S.K, Dedeepya Y, Al-Aidroos H.J, Reddy M.V.K (2019) Design And Analysis Of Flying Wing UAV Using XFLR5. International Journal Of Advancements In Mechanical And Aeronautical Engineering. Vol 6, Iss 1. ISSN: 2372-4153
- [8] Sharma S, Sharieff U, Singh A, Tarnacha R.S (2021) Design And Fabrication Of Fixed-Wing UAV For Commercial Monitoring. International Research Journal Of Engineering And Technology. Vol 08, Iss 08, Pg 1153-117. ISSN: 2395-0072
- [9] Raymer D.P (1989) Aircraft Design: A Conceptual Approach. AIAA Education Series, Washington, DC.